


# Inhibition of tumor formation and metastasis by a monoclonal antibody against lymphatic vessel endothelial hyaluronan receptor 1

Yuta Hara<sup>1</sup> | Ryota Torii<sup>1</sup> | Shiho Ueda<sup>1</sup> | Erina Kurimoto<sup>1</sup> | Eri Ueda<sup>1</sup> | Hiroshi Okura<sup>1</sup> | Yutaka Tatano<sup>2</sup> | Hideki Yagi<sup>2</sup> | Yoshiya Ohno<sup>3</sup> | Toshiyuki Tanaka<sup>3</sup> | Kazue Masuko<sup>1</sup> | Takashi Masuko<sup>1</sup> 

<sup>1</sup>Cell Biology Laboratory, School of Pharmacy, Kindai University, Higashiosaka, Osaka, Japan

<sup>2</sup>Department of Pharmaceuticals, Faculty of Pharmacy, International University of Health and Welfare, Otawara, Tochigi, Japan

<sup>3</sup>Laboratory of Immunobiology, Department of Pharmacy, School of Pharmacy, Hyogo University of Health Sciences, Kobe, Hyogo, Japan

**Correspondence:** Takashi Masuko, Cell Biology Laboratory, School of Pharmacy, Kindai University, Higashiosaka-shi, Japan (masuko@phar.kindai.ac.jp).

## Funding information

A matching fund subsidy-supported Program for the Strategic Research Foundation at Private Universities (2014-2018), Grant/Award Number: S1411037; "Academic Frontier" Project (Kindai University, 2005-2007), Grant/Award Number: F000132; "Adaptable and Seamless Technology Transfer Program through R&D" Project (2009-2011), Grant/Award Number: AS2115048G

## Abstract

Although cancer metastasis is associated with poor prognosis, the mechanisms of this event, especially via lymphatic vessels, remain unclear. Lymphatic vessel endothelial hyaluronan receptor 1 (LYVE-1) is expressed on lymphatic vessel endothelium and is considered to be a specific marker of lymphatic vessels, but it is unknown how LYVE-1 is involved in the growth and metastasis of cancer cells. We produced rat monoclonal antibodies (mAb) recognizing the extracellular domain of mouse LYVE-1, and investigated the roles of LYVE-1 in tumor formation and metastasis. The mAb 38M and 64R were selected from hybridoma clones created by cell fusion between spleen cells of rats immunized with RH7777 rat hepatoma cells expressing green fluorescent protein (GFP)-fused mouse LYVE-1 proteins and mouse myeloma cells. Two mAb reacted with RH7777 and HEK293F human embryonic kidney cells expressing GFP-fused mouse LYVE-1 proteins in a GFP expression-dependent manner, and each recognized a distinct epitope. On immunohistology, the 38M mAb specifically stained lymphatic vessels in several mouse tissues. In the wound healing assay, the 64R mAb inhibited cell migration of HEK293F cells expressing LYVE-1 and mouse lymphatic endothelial cells (LEC), as well as tube formation by LEC. Furthermore, this mAb inhibited primary tumor formation and metastasis to lymph nodes in metastatic MDA-MB-231 xenograft models. This shows that LYVE-1 is involved in primary tumor formation and metastasis, and it may be a promising molecular target for cancer therapy.

## KEYWORDS

lymphangiogenesis, lymphatic metastasis, lymphatic vessel endothelial hyaluronan receptor 1, monoclonal antibody, primary tumor

Hara and Torii equally contributed to this study.

This is an open access article under the terms of the Creative Commons Attribution-NonCommercial License, which permits use, distribution and reproduction in any medium, provided the original work is properly cited and is not used for commercial purposes.

© 2018 The Authors. *Cancer Science* published by John Wiley & Sons Australia, Ltd on behalf of Japanese Cancer Association.

## 1 | INTRODUCTION

Cancer metastasis is associated with poor prognosis and accounts for the majority of cancer-related deaths.<sup>1-3</sup> There are 2 major mechanisms by which cancer metastasis occurs: hematogenous and lymphogenous metastasis.<sup>4,5</sup> The lymphatic route has been shown to be more important as an initial route for the spread of cancer than the hematogenous route,<sup>6,7</sup> especially for carcinomas (epithelial cancers). Accordingly, metastatic spread to lymph nodes (LN) is regarded as a prognostic indicator,<sup>8</sup> but the details of the mechanism of lymphogenous metastasis are unclear.

Lymphatic vessel endothelial hyaluronan receptor 1 (LYVE-1) is a homolog of cluster of differentiation (CD) 44, a receptor for hyaluronan expressed on lymphatic endothelial cells (LEC),<sup>9,10</sup> and is utilized as a lymphatic-specific marker. LYVE-1 binds to hyaluronan, and is involved in the migration of LEC,<sup>11,12</sup> as well as in the transport of hyaluronan to the liver and regional LN.<sup>13</sup> Furthermore, LYVE-1 promotes hyaluronan-induced lymphangiogenesis.<sup>11,14</sup> In clinical studies, LYVE-1 proteins were significantly increased in colon tumors compared with in unaffected colon tissues.<sup>15</sup> LYVE-1 gene expression was upregulated in muscle-invasive bladder cancers exhibiting positive lympho-vascular invasion and LN metastasis compared with in non-muscle invasive bladder cancers.<sup>16</sup> In a xenograft mouse model, intratumoral and peritumoral LYVE-1-positive vessels increased in vascular endothelial growth factor (VEGF)-C-overexpressing breast cancer cells.<sup>17,18</sup> These findings suggest that LYVE-1 is a potential target for cancer therapy, but it is not known whether cancer therapy targeting LYVE-1 can improve primary cancer formation, tumor progression or cancer metastasis.

In this study, we produced novel anti-mouse LYVE-1 rat monoclonal antibodies (mAb), and found them to be useful tools for the treatment of human cancers.

## 2 | MATERIALS AND METHODS

### 2.1 | Animals

Female F344/N rats, male BALB/c mice, and male KSN nude mice were purchased from Shimizu Animal Farm (Kyoto, Japan), and male SCID mice were purchased from Japan SLC (Hamamatsu, Japan) at 6 weeks of age. All animals were maintained in specific pathogen-free conditions. They were housed individually in plastic cages under a standard light/dark cycle (12-hour light cycle starting at 07:00 hours) at a constant temperature of  $23 \pm 1^\circ\text{C}$ , and had ad libitum access to food and water. All animal experiments in the present study were approved by the Committee for the Care and Use of Laboratory Animals at Kindai University (KAPS-23-004, KAPS-26-019 and KAPS-27-006), and performed following the institutional guidelines.

### 2.2 | Transfectants expressing LYVE-1

Mouse LYVE-1 cDNA was reverse transcribed with a First Strand cDNA Synthesis kit (GE Healthcare, Chicago, IL, USA) from total RNA prepared by Isogen II (Nippon Gene, Toyama, Japan) of mouse

stomach tissues rich in lymphatic vessels. Green fluorescent protein (GFP) was fused to the carboxy terminus of full-length (membrane form) or the extracellular domain (secretory form) of mouse LYVE-1 in the pAcGFP vector (BD Biosciences, Mountain View, CA, USA). Transfection of the full-length or secretory mouse LYVE-1-GFP vector into cells was performed using Lipofectamine 3000 (Invitrogen, Carlsbad, CA, USA) according to the manufacturer's instructions. Cells were selected using culture media containing 400  $\mu\text{g}/\text{mL}$  G418 (Nacalai Tesque, Kyoto, Japan), and were sorted by cellular green fluorescence using a JSAN cell sorter (Bay Bioscience, Kobe, Japan). These experiments were approved by the Safety Committee for Recombinant DNA Experiments at Kindai University (KDPS-19-002, KDPS-21-001 and KDPS-26-004).

### 2.3 | Cell culture

Cell lines originated from rat hepatoma (RH7777, donated by Dr K Chiba, Tanabe Mitsubishi Pharm, Tokyo, Japan), mouse myeloma (P3X63Ag8.653, purchased from American Type Cell Collection [ATCC], Manassas, VA, USA), human embryonic kidney (HEK293F, purchased from Invitrogen), human breast cancer (MDA-MB-231-luc-LN, hereinafter called MDA-231, provided by Shionogi Pharm, Osaka, Japan) and mouse LN endothelium (SVEC4-10,<sup>19</sup> purchased from ATCC) were cultured in RD medium, which is a 1:1 mixture of Dulbecco's modified Eagle's medium and RPMI-1640 medium (Nissui Pharmaceutical, Tokyo, Japan) supplemented with 7% heat-inactivated fetal bovine serum (FBS, Thermo Fisher Scientific, Waltham, MA, USA), in humidified  $\text{CO}_2$  incubators. RH7777 or HEK293F transfectants expressing full-length mouse LYVE-1-GFP were cultured in RD medium. HEK293F cells expressing and secreting soluble mouse LYVE-1-GFP proteins were cultured in FreeStyle293 expression medium (Invitrogen), and culture supernatants obtained following centrifugation at  $1000\times g$  were used as soluble mouse LYVE-1 proteins for mAb screening by enzyme-linked immunosorbent assay (ELISA).

### 2.4 | Production of rat mAb against mouse LYVE-1

Production of anti-LYVE-1 mAb was carried out according to our previous reports.<sup>20-22</sup> RH7777 rat hepatoma cells expressing mouse LYVE-1 fused to GFP ( $2 \times 10^7$  cells) were given s.c. (first immunization), i.p. (second and third immunizations) and i.v. (final immunization) into F344/N rats every 4 weeks. Three days after the last immunization, the spleen cells ( $1 \times 10^8$  cells) were fused with P3X63Ag8.653 mouse myeloma cells ( $2.5 \times 10^7$  cells) with 50% polyethylene glycol (Roche, Basel, Switzerland). Hybridomas were selected using RPMI-1640 containing hypoxanthine, aminopterin and thymidine (HAT, 50 $\times$  solution, Invitrogen) with 7% FBS, and were selected based on the reactivity of mAb against soluble or cell-bound mouse LYVE-1 by ELISA and flow cytometry (FCM), respectively. Selected hybridoma cells were cloned using the limiting-dilution method, and hybridoma clones ( $3 \times 10^6$  to  $1 \times 10^7$  cells) were injected i.p. into KSN nude mice pretreated i.p. with

2,6,10,14-tetramethylpentadecane (Pristane; Wako Pure Chemical Industries, Osaka, Japan). Approximately 8–16 days after administration, ascites fluid was collected, and the mAb were purified using Protein G Sepharose (BD Healthcare, Uppsala, Sweden). The isotype of mAb, namely heavy chain (sub) classes and light chain types, was determined using the Rapid Monoclonal Antibody Isotyping Kit (Antigen Pharmaceuticals, Boston, MA, USA). Phycoerythrin (PE)-conjugated anti-mouse LYVE-1 mAb were prepared using the R-Phycoerythrin conjugation Kit (Abcam, Cambridge, UK, ab102918).

## 2.5 | Enzyme-linked immunosorbent assay

Soluble mouse LYVE-1 fused to GFP or soluble mouse CD44<sup>23,24</sup> fused to GFP was adsorbed to the wells in polyvinyl chloride 96-well plates (E-type, Sumitomo Bakelite, Tokyo, Japan) overnight at 4°C. Each well was treated with Block Ace (Dainihon Seiyaku, Osaka, Japan) for 1 hour at 37°C, and then hybridoma culture supernatants (undiluted) or purified antibody (38M or 64R: 10 µg/mL) were added to each well. One hour after the incubation at room temperature (RT), 1:2000 diluted horseradish peroxidase (HRP)-conjugated rabbit anti rat IgG polyclonal antibody (pAb; Dako Japan, Tokyo, Japan) was added and incubated for 1 hour at RT. After extensive washing of each well with phosphate-buffered saline (PBS, pH 7.5) containing 0.05% Tween 20, substrate solution (SureBlue TMB substrate, KPL, Gaithersburg, MD, USA) was added to each well and the enzyme reaction was stopped by the addition of 0.5 mol/L H<sub>2</sub>SO<sub>4</sub>. The optical density of the solution in each well was measured using a Model 550 plate reader (Bio-Rad, Hercules, CA, USA).

## 2.6 | Immunoprecipitation and SDS-PAGE

Cells ( $5.0 \times 10^6$  cells) were suspended in modified PBS (pH 8.0) containing 0.5 mg/mL sulfosuccinimidyl-6'-(biotinamide)-6-hexanoamide hexanoate (EZ-Link sulfo-NHS-LC-LC-Biotin; Thermo Fisher Scientific), and incubated for 30 minutes at RT. The cells were treated with lysis buffer (50 mmol/L Tris-HCl (pH 7.4), 150 mmol/L NaCl, 1% Nonidet P-40 and protease inhibitor cocktail [Nacalai Tesque]) for 20 minutes at 4°C. After centrifugation at  $20\,000 \times g$  for 10 minutes, the supernatant was collected as the cell lysate, incubated with 20 µg anti-mouse LYVE-1 mAb (38M or 64R) at 4°C overnight, and were mixed with Protein G Sepharose 4 Fast Flow (GE Healthcare) at 4°C for 4 hours. After centrifugation at  $9000 \times g$  for 20 seconds, precipitates were incubated with SDS sample buffer (45 mmol/L Tris-HCl [pH 6.8], 10% glycerol, 1% SDS, 0.01% bromophenol blue and 0.05 mol/L DTT) for 3 minutes at 95°C. The proteins were separated using SDS-PAGE (8%), and transferred to polyvinylidene fluoride membranes (Immobilon-P, Millipore, Billerica, MA, USA). The membranes were reacted with Elite avidin-biotin-peroxidase complex (ABC) solution (Vector Laboratories, Burlingame, CA, USA). Protein bands were detected using Chemi-Lumi One Super (Nacalai Tesque) and the ImageQuant RT ECL Imager (GE Healthcare).

## 2.7 | Flow cytometry

Cells ( $1 \times 10^5$ – $5 \times 10^5$  cells) were inoculated into each well of a 96-well plate, and hybridoma culture supernatants (without dilution) or purified mAb (10 µg/mL) were added. Sixty minutes after the incubation at 4°C, cells were incubated with 1:300 diluted PE-labeled donkey anti-rat IgG (H+L; Jackson ImmunoResearch, West Grove, PA, USA) for 30 minutes at 4°C. For 2-color immunostaining of SVEC4-10, cells fixed by 4% paraformaldehyde (PFA; Wako Pure Chemical Industries) were treated with combinations of anti-LYVE-1 (38M or 64R, 10 µg/mL) rat mAb and anti-LYVE-1 (Abcam, ab14917) rabbit pAb (1:100 diluted) for 60 minutes at 4°C. Following extensive washing of cells with PBS, they were treated with 1:200 diluted species-specific Alexa Fluor 488-conjugated anti-rat IgG (H+L) and Alexa Fluor 647-conjugated anti-rabbit IgG (H+L) donkey pAb (Jackson ImmunoResearch) for 45 minutes at 4°C. For the competitive binding inhibition assay, HEK293F cells expressing mouse LYVE-1 were incubated with 400 µg/mL unlabeled anti-LYVE-1 mAb and 10 µg/mL PE-labeled anti-LYVE-1 mAb for 1 hour at 4°C. After extensive washing, cells were suspended in 0.2% BSA-PBS, and the fluorescence intensity of individual cells was measured using an Accuri C6 or LSR Fortessa flow cytometer (Becton-Dickinson, Franklin Lakes, NJ, USA). Based on the mean fluorescence intensity (MFI) with or without primary mAb, the subtracted ( $\Delta$ ) MFI or the ratio (+mAb/–mAb) of MFI (rMFI) was calculated. On competitive binding inhibition, the % binding inhibition was calculated using the MFI of PE-labeled 38M or 64R with or without excess unlabeled mAb.

## 2.8 | Isolation of primary LEC and FCM

The LEC isolation was performed as previously reported.<sup>25,26</sup> LN (mesenteric, inguinal, axillary, and submandibular) were removed from BALB/c mice, and minced LN were immersed into medium containing 100 µg/mL DNase I (Sigma-Aldrich, St Louis, MO, USA), 25 µg/mL Liberase (Sigma-Aldrich), 2% FBS and 10 mmol/L HEPES, and incubated at 37°C for 20 minutes. Samples were passed through a glass Pasteur pipet several times. Digestion was stopped by the addition of 10 mmol/L EDTA. The remaining aggregates were further digested with new enzyme solution. The samples were stained with fluorescein isothiocyanate (FITC)-labeled anti-CD45 (Miltenyi Biotec, Bergisch Gladbach, Germany), PE-labeled 38M or 64R and 4',6-diamidino-2-phenylindole (DAPI, 0.5 µg/mL; Wako Pure Chemical Industries). PFA (4%)-fixed samples were stained with FITC-labeled anti-CD45 and anti-LYVE-1 rabbit pAb, followed by incubation with Alexa Fluor 647-conjugated anti-rabbit IgG donkey pAb.

## 2.9 | Immunoperoxidase staining of mouse tissues

Mice were anesthetized with isoflurane (Wako) and each organ was isolated. Organs were embedded in OCT Compound (Sakura Finetek Japan, Tokyo, Japan) in liquid nitrogen. Tissue sections (7 µm) were obtained using a cryostat (CM1800, Leica Microsystems, Wetzlar, Germany) and mounted on poly-L-lysine (PLL)-coated slides. Tissue

sections were fixed by 4% PFA and treated with Block Ace overnight. Sections were incubated with 10  $\mu\text{g}/\text{mL}$  38M or 64R for 60 minutes at RT. After a 5-minute treatment with 3%  $\text{H}_2\text{O}_2$  in methanol, sections were incubated with 1:1000 diluted biotinylated rabbit anti-rat IgG (H+L; Jackson ImmunoResearch) for 60 minutes at RT. They were subsequently reacted with 1:100 diluted Elite ABC solution (Vector) for 30 minutes and substrate 3,3'-diaminobenzidine (DAB, Dojin, Chemicals, Kumamoto, Japan) solution. Finally, they were counterstained with Methyl Green (Merck, Darmstadt, Germany). The localization of antibody-defined components (LYVE-1) was observed using a Zeiss Axiolab microscope (Carl Zeiss, Oberkochen, Germany).

## 2.10 | Confocal analysis of mouse tissues

Mouse tissue sections prepared as described in the previous section were treated with combinations of anti-LYVE-1 (38M, 5  $\mu\text{g}/\text{mL}$ ) rat mAb and anti-LYVE-1 or anti-CD31 rabbit pAb (1:100 diluted) overnight at RT. After extensive washing with PBS, tissue sections were treated with 1:200 diluted species-specific Alexa Fluor 488-conjugated anti-rat IgG (H+L) and Alexa Fluor 647-conjugated anti-rabbit IgG (H+L) donkey pAb (Jackson ImmunoResearch) for 60 minutes at RT. The localization of antibody-defined components was observed on confocal laser fluorescence microscopy with FV10C-O (Olympus, Tokyo, Japan).

## 2.11 | Wound healing assay

The HEK293F cells expressing mouse LYVE-1-GFP or SVEC4-10 cells were plated onto plastic dishes. When the cells neared 100% confluency, scratch wounds were made by scraping the cell layer with a micropipette tip. Supernatants from MDA-231 cells were then added to the wounded cultures with or without anti-LYVE-1 mAb. Images of each scratch wound were taken using a Zeiss Axiolab microscope (Carl Zeiss).

## 2.12 | In vitro tube formation assay

The tube formation assay was performed as previously reported.<sup>14,27</sup> Matrigel (Corning, Corning, NY, USA) was added to each well (130  $\mu\text{L}$ ) of an 8-well slide chamber (WATSON Bio Lab, Kobe, Japan), and allowed to solidify at 37°C for 30 minutes. SVEC4-10 cells ( $5 \times 10^4$  cells) in RD medium supplemented with 7% FBS and supernatants from MDA-231 cells were added, and incubated in humidified  $\text{CO}_2$  incubators for 3 hours. Images were taken using a Zeiss Axiolab microscope (Carl Zeiss).

## 2.13 | In vivo bioluminescence imaging of tumors

MDA-MB-231-Luc-LN cells ( $4 \times 10^6$  cells) were implanted into the mammary fat pads of SCID mice. After visual confirmation of tumor engraftment, 64R or control ascites fluid (500  $\mu\text{L}/\text{mouse}$ ) was injected i.p. into each mouse 4 times every 4 days.

D-Luciferin (150 mg/kg body weight; Wako) was administered to mice 10 minutes prior to imaging. Mice were anesthetized with isoflurane and imaged using an in vivo imaging system (IVIS Lumina XRMS Series III, PerkinElmer, Waltham, MA, USA). Images were analyzed using Living Image (Xenogen, Alameda, CA, USA). The bioluminescence flux (photons/s/sr/cm<sup>2</sup>) was measured for the axillary LN and primary tumors.

## 2.14 | In vivo anti-tumor effects of mAb in primary tumor formation

Nude mice were inoculated intradermally with MDA-231 ( $4 \times 10^6$  cells) 24 hours after i.p. treatment with TM- $\beta$ 1 anti-mouse IL-2 receptor  $\beta$  chain mAb<sup>28</sup> (300  $\mu\text{g}/\text{mouse}$ ). After visual confirmation of tumor engraftment, 64R or isotype control IgG mAb (250  $\mu\text{g}/\text{mouse}$ ) was injected i.p. into each mouse 4 times every 4 days. The size of each tumor was periodically measured, and the tumor volume (mm<sup>3</sup>) was calculated using the formula  $0.5 \times (\text{length}) \times (\text{width})^2$ .

## 2.15 | Statistical analysis

Data are expressed as mean  $\pm$  SEM. Data for the wound healing assay were analyzed using 1-way analysis of variance (ANOVA) followed by Tukey's post-hoc multiple comparison test. Data from the xenograft model were analyzed with the Mann-Whitney *U*-test or Student's *t*-test. Statistical analysis was carried out with Prism 7 for Windows (GraphPad, San Diego, CA, USA). The criterion for significance was  $P < .05$ .

# 3 | RESULTS

## 3.1 | Production of rat mAb against mouse LYVE-1

Expression plasmids encoding cDNA of GFP-fused mouse LYVE-1 (GFP-LYVE-1) were transfected into RH7777 rat hepatoma cells, and stable transfectant clones were established by G418-selection and cell sorting. Rats were immunized with these transfectant clones 4 times, and splenocytes obtained from the immunized rats were fused with mouse myeloma cells. As the first screening, we examined the reactivity of the antibodies in the supernatants of hybridomas with the GFP-fused soluble extracellular domain of mouse LYVE-1 on ELISA, and then selected 64 hybridoma cell lines that secreted anti-LYVE-1 mAb (Figure 1A). Next, we evaluated the specificity of the anti-LYVE-1 mAb that we selected in the first screening on the second screening with FCM. Two mAb, designated 38M (IgG<sub>2a</sub>/ $\kappa$ ) and 64R (IgG<sub>2a</sub>/ $\kappa$ ), strongly reacted with LYVE-1-expressing RH7777 and HEK293F cells in a GFP expression level-dependent manner (Figure 1B). Furthermore, these mAb did not bind to the secretory form of mouse CD44 hyaluronan receptor, which is functionally and structurally related to LYVE-1 (Figure 1C). On immunoprecipitation analysis, both 38M and 64R immunoprecipitated 87-kDa proteins (GFP-fused LYVE-1) in extracts prepared from surface-biotinylated GFP-LYVE-1-expressing HEK293F cells (Figure 1D).

We then examined whether 38M and 64R recognize the same epitope using a competitive binding inhibition assay on FCM (Figure 2). The reactivity of PE-labeled 38M against HEK293 cells expressing mouse LYVE-1 was significantly reduced with excess unlabeled 38M (88.5% binding inhibition) but not with 64R (9.3%), and that of PE-labeled 64R was reduced with unlabeled 64R (93.1%) but not with 38M (7.7%; Figure 2), demonstrating that each mAb recognizes a different epitope on the extracellular domain of mouse LYVE-1.

We analyzed the effects of cell fixation on the reactivity of anti-LYVE-1 mAb. Although both 38M and 64R mAb retained reactivity with HEK293F cells expressing mouse LYVE-1 after treatment with 4% PFA, the MFI decreased to 72.8% (38M) and 52.4% (64R) of that of unfixed living cells (100%), indicating that the epitope recognized by 64R is more sensitive to PFA fixation than that recognized by 38M (data not shown).

We next evaluated the reactivity of our mAb with primary mouse LEC (Figure 3A) and the SVEC4-10 LEC line (Figure 3B-D). Anti-LYVE-1 rabbit pAb reacted with approximately one-fourth of the CD45<sup>-</sup> non-hematopoietic cells isolated from mouse LN. 38M and 64R also reacted with 29% (38M) and 17% (64R) of DAPI-

unstained and CD45<sup>-</sup> viable non-hematopoietic cells, respectively. The SVEC4-10 mouse LEC cells were definitely reactive with 38M, 64R, and anti-LYVE-1 rabbit pAb, but faintly with anti-CD31 rabbit pAb (Figure 3B,C). All 38M<sup>+</sup> and 64R<sup>+</sup> cell populations were detected in SVEC4-10 cells stained with anti-LYVE-1 rabbit pAb (Figure 3D).

### 3.2 | Expression of LYVE-1 in lymphatic vessels of various mouse tissues

Given that LYVE-1 is expressed on endothelial cells of lymphatic vessels, we immunostained the axillary LN in mice with 38M and 64R. On immunohistochemical analysis, 38M and 64R stained lymphatic vessels (Figure 4A). Given that the immunostaining signals of 38M were stronger than those of 64R (Figure 4A), we next examined the reactivity of 38M in different tissues, such as gastrointestinal (esophagus, stomach, cecum), respiratory (lung, trachea), cardiovascular (heart), muscle (tongue), skin (ear), and lymphoid (nose) tissues, and found that 38M reacted with lymphatic vessels in all tested mouse tissues (Figure 4B).

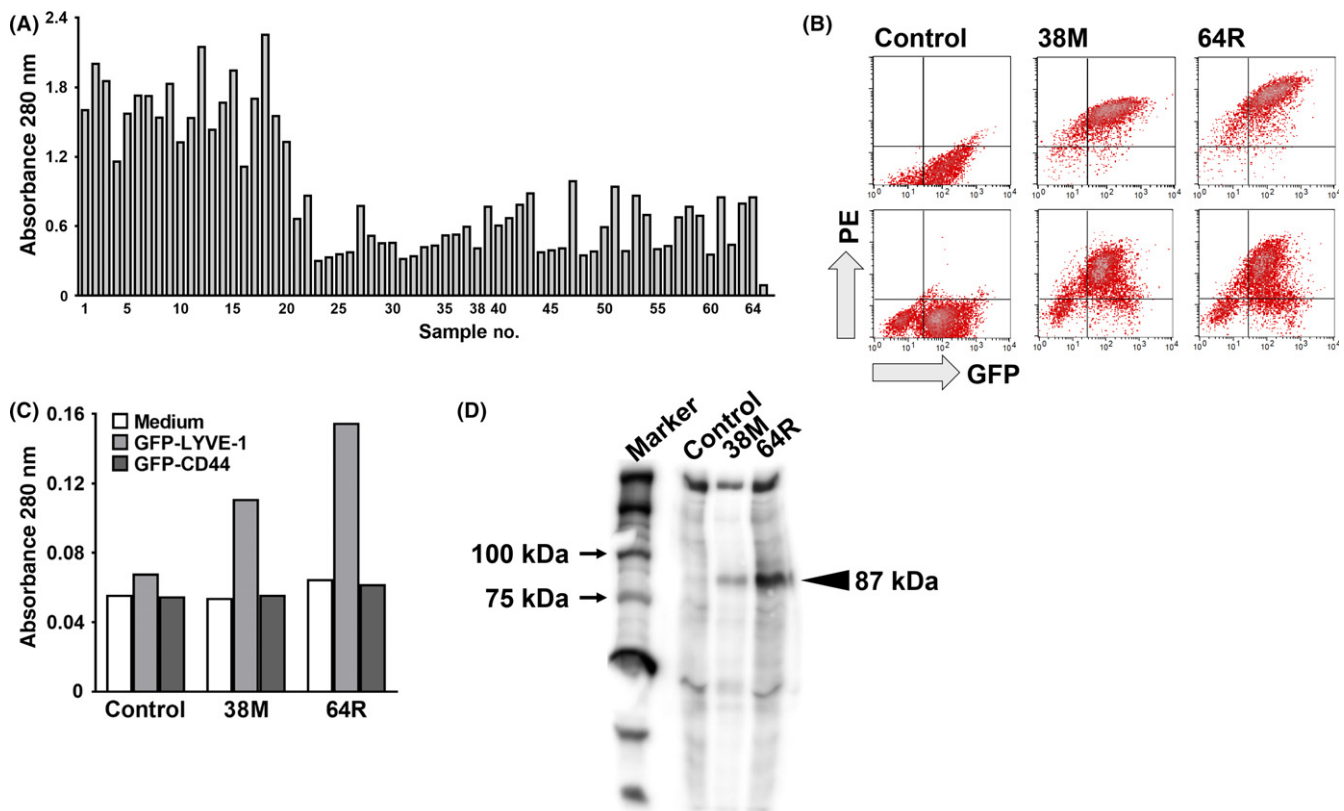


**FIGURE 1** Production and characterization of anti-mouse lymphatic vessel endothelial hyaluronan receptor 1 (LYVE-1) rat monoclonal antibodies (mAb). A, First screening: 64 hybridoma clones with strong reactivity to soluble LYVE-1 proteins fused to GFP on ELISA. Samples 38 (38M) and 64 (64R) are the clones selected in the 2nd screening. Sample 65, control (right end, mAb-). B, Second screening: flow cytometry analysis of the 38M and 64R mAb against GFP-LYVE-1-expressing HEK293F (upper) and RH7777 (lower). PE, phycoerythrin. C, Reactivity of the 38M and 64R mAb with serum-free culture supernatants from HEK293F cells transfected with GFP-LYVE-1 or GFP-CD44 on ELISA. D, SDS-PAGE of HEK293F cells transfected with GFP-LYVE-1, and surface-biotinylated and immunoprecipitated with anti-mouse LYVE-1 rat mAb. Proteins were visualized with Elite ABC and peroxidase substrates. Arrowheads, positions of mAb-bound GFP-mouse LYVE-1 proteins

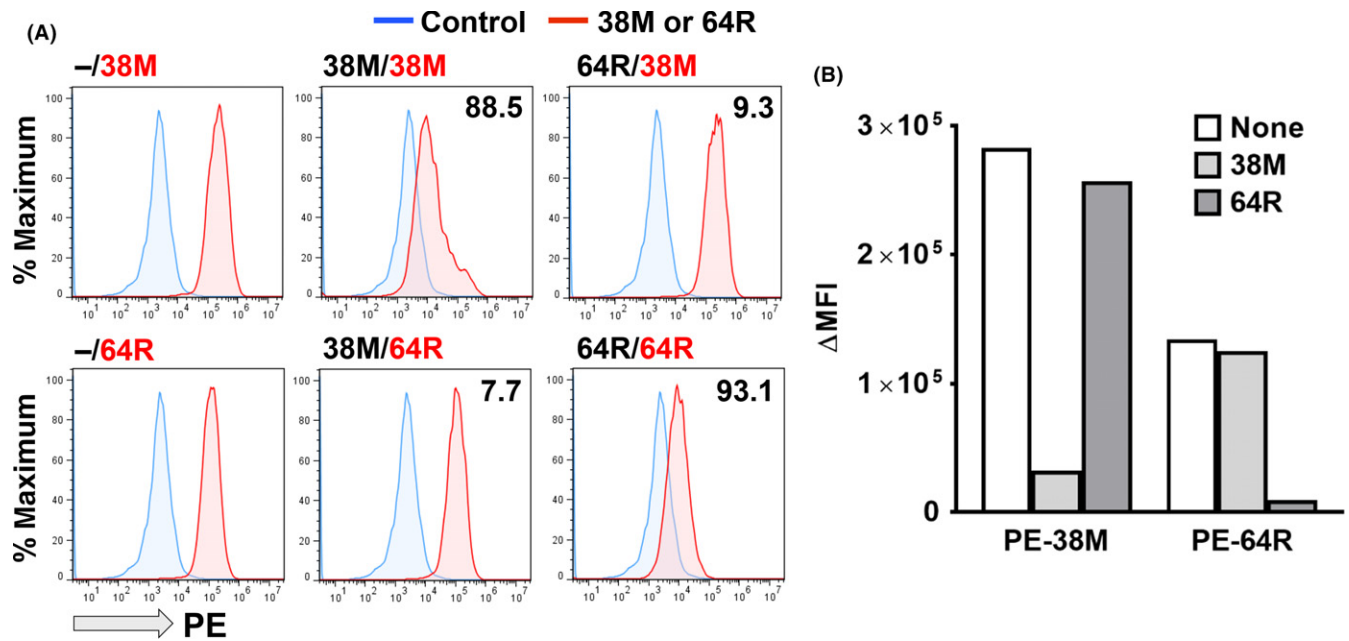


**FIGURE 2** Difference in epitopes recognized by 38M and 64R. A, Phycoerythrin (PE)-associated fluorescence of HEK293F cells expressing mouse lymphatic vessel endothelial hyaluronan receptor 1 (LYVE-1) incubated with PE-labeled anti-LYVE-1 mAb with or without excess unlabeled anti-LYVE-1 mAb (38M or 64R) on flow cytometry. Panel labels, unlabeled mAb/PE-labeled mAb. Number in each panel, % binding inhibition. B, Subtracted ( $\Delta$ ) mean fluorescence intensity (MFI), reactivity of PE-labeled mAb with or without excess unlabeled mAb

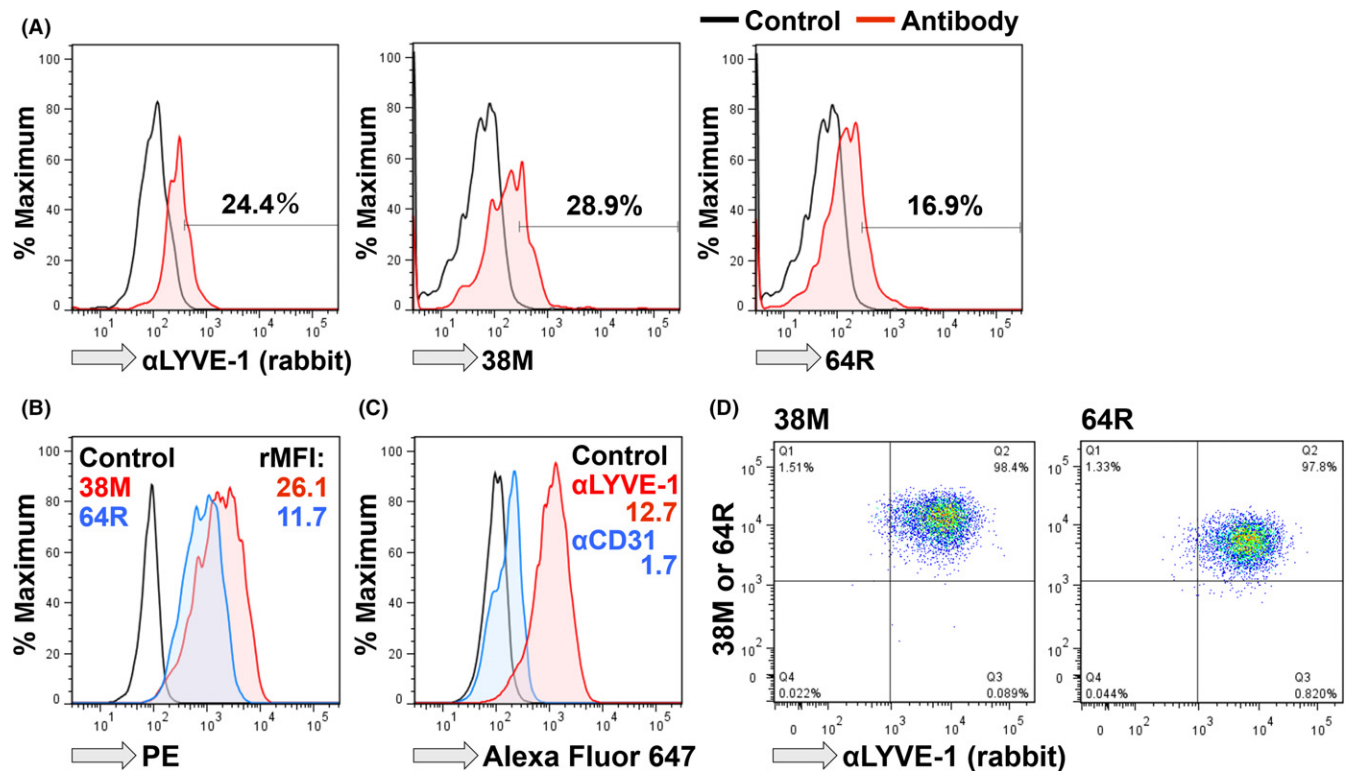


**FIGURE 3** Reactivity of anti-lymphatic vessel endothelial hyaluronan receptor 1 ( $\alpha$ LYVE-1) mAb with mouse lymphatic endothelial cells (LEC). A, Samples were collected from mouse lymph nodes (LN), and CD45<sup>-</sup> cells were analyzed. (left) Paraformaldehyde (PFA)-fixed cells were stained with  $\alpha$ LYVE-1 rabbit polyclonal antibodies (pAb), and CD45<sup>-</sup> and DAPI-unstained viable cells were stained with middle (38M) or (right) 64R rat mAb. B, SVEC4-10 LEC were analyzed for reactivity with 38M and 64R. C, SVEC4-10 LEC were analyzed for reactivity with pAb. D, SVEC4-10 cells were stained with a combination of  $\alpha$ LYVE-1 rabbit pAb and 38M or 64R. PE, phycoerythrin

### 3.3 | Expression of LYVE-1 on the surface of lymphatic vessels but not blood vessels

To confirm LYVE-1 as a specific marker of lymphatic vessels, we compared the localization of CD31 and LYVE-1 in mouse stomach tissue from which mouse LYVE-1 cDNA was obtained (Figure 5). First, we examined the co-localization of LYVE-1 stained with 38M anti-mouse LYVE-1 rat mAb and the anti-mouse LYVE-1 rabbit pAb available on the market. Based on 2-color immunostaining followed by confocal analysis, the components stained with both antibodies were completely matched and merged on the endothelia of lymphatic vessels, confirming the specificity of our rat mAb (Figure 5, upper panels). Next, we performed 2-color immunostaining of mouse stomach tissues with 38M and rabbit pAb recognizing mouse CD31, which is a specific marker of blood vessels. On confocal microscopy analysis, the components stained with both antibodies were completely separated, demonstrating the reactivity of 38M mAb against LYVE-1 to be a specific marker of lymphatic vessels (Figure 5, lower panels).

### 3.4 | Effects of anti-LYVE-1 mAb on the migration of LYVE-1-positive cells

Lymphangiogenesis is associated with cancer metastasis,<sup>29</sup> and the migration of LEC is an important step in the early phase of lymphangiogenesis.<sup>30,31</sup> Thus, we examined whether the anti-LYVE-1 mAb suppressed the migration of HEK293F cells expressing mouse LYVE-1 proteins on the wound healing assay. Induction of cell migration, which was facilitated by the supernatant from MDA-231 cells, was significantly suppressed by the 64R mAb in a dose-dependent manner (Figure 6A,B). In contrast, there was no difference in the migration speed between mAb-treated cells and control cells in the absence of the supernatant (data not shown). Furthermore, MDA-231 cell-facilitated migration of SVEC4-10 mouse LEC, which endogenously express LYVE-1 proteins, was also inhibited by anti-LYVE-1 mAb in a dose-dependent manner (Figure 6C).

Given that tube formation of LEC is a known aspect of lymphangiogenesis,<sup>11,32</sup> we next examined the effects of our anti-LYVE-1 mAb on tube formation of SVEC4-10 mouse LEC. Tube formation of

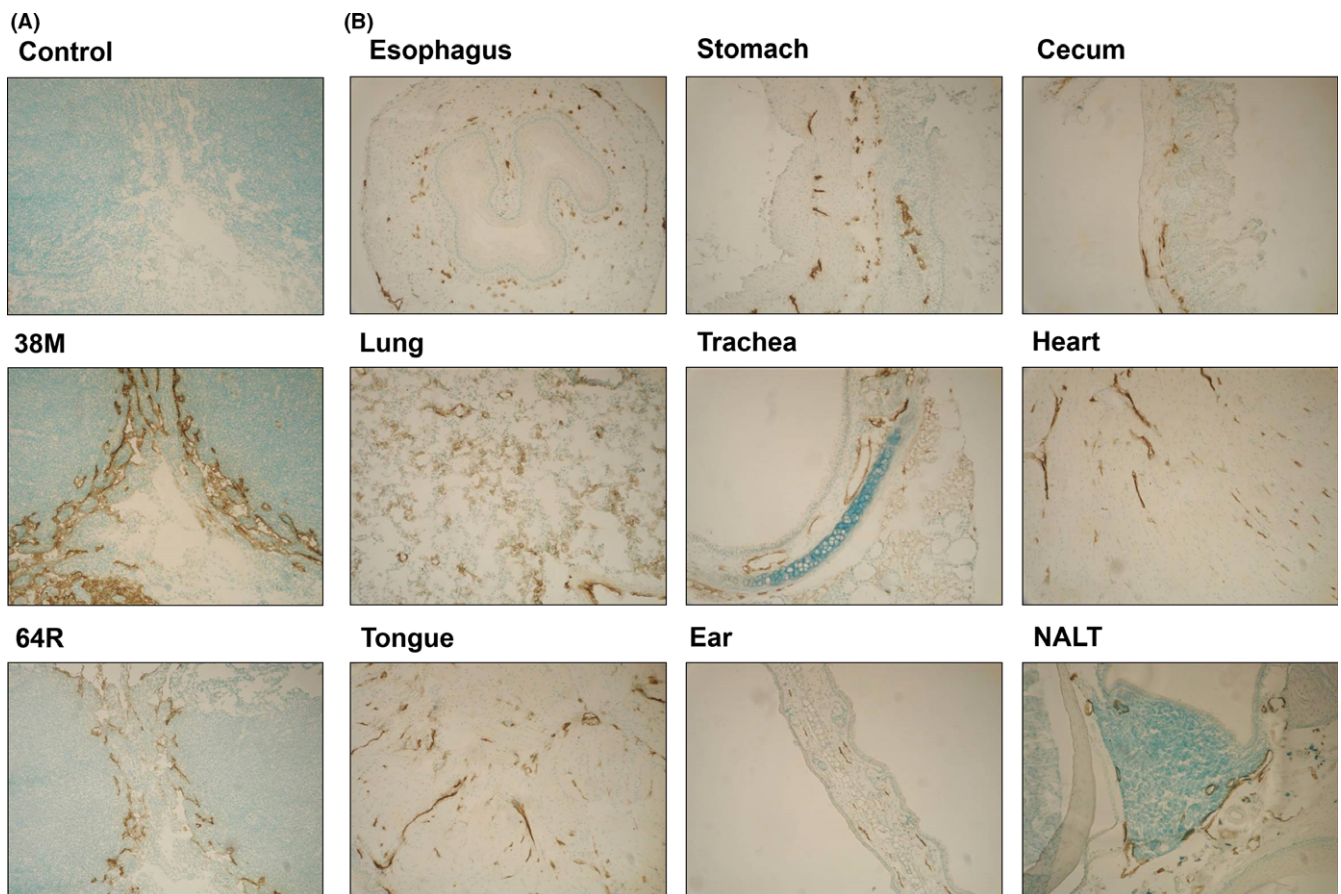


**FIGURE 4** Reactivity of anti-lymphatic vessel endothelial hyaluronan receptor 1 (anti-LYVE-1) mAb with normal mouse tissues. A, Paraformaldehyde (PFA)-fixed tissues from mouse axillary lymph nodes stained using the immunoperoxidase method with 38M or 64R rat mAb. B, PFA-fixed mouse lymphatic vessels in various organs stained with 38M rat mAb. Nuclei were counterstained with methyl green. NALT, nasal-associated lymphoid tissue

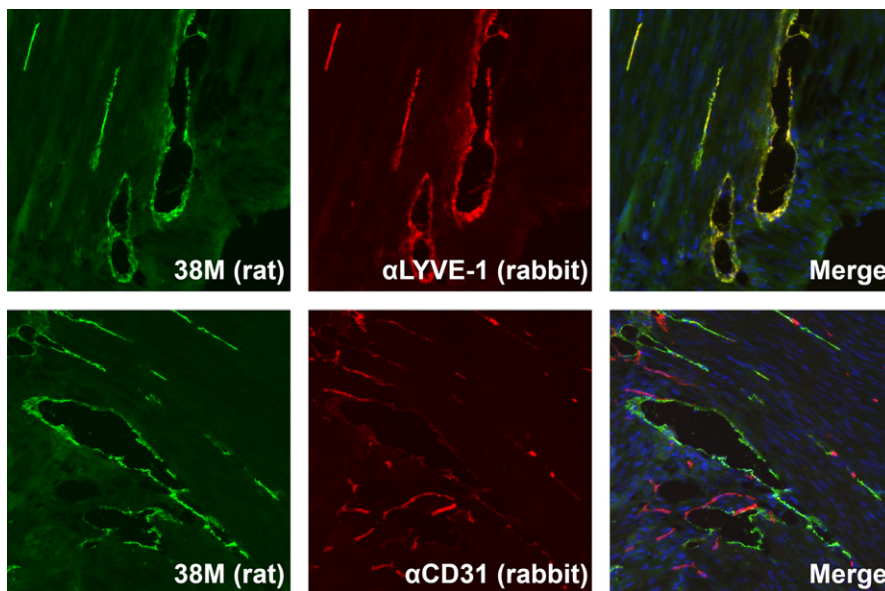


**FIGURE 5** Confocal analysis of lymphatic vessel endothelial hyaluronan receptor 1 (LYVE-1) in mouse stomach tissue. Paraformaldehyde (PFA)-fixed mouse tissue sections were treated with the 38M rat mAb in combination with anti-LYVE-1 or anti-CD31 rabbit antibodies overnight at room temperature. Tissue sections were treated with species-specific Alexa Fluor 488-conjugated anti-rat and Alexa Fluor 678-conjugated anti-rabbit IgG for 60 minutes at room temperature. The localization of antibody-defined components (LYVE-1 and CD31) was observed using a confocal microscope

LEC in the presence of the supernatant from MDA-231 cells was significantly inhibited by 64R (Figure 6D).

### 3.5 | Effects of anti-LYVE-1 mAb on LN metastasis of cancer cells

MDA-MB-231-luc-LN breast cancer cells were orthotopically inoculated into inguinal mammary glands of SCID mice, and primary tumor and cell metastasis to LN were monitored on bioluminescence imaging. The bioluminescence of luciferase was detected in not only the primary lesion, but also in ipsilateral and contralateral axillary LN (Figure 7A). We investigated whether inhibition of LYVE-1 can suppress cancer metastasis using ascites fluid obtained from the mice harboring 64R anti-LYVE-1 mAb-secreting hybridoma cells. The ascites fluid significantly reduced the bioluminescence intensity in axillary LN (Figure 7B). In contrast, although the bioluminescence intensity in the primary tumor decreased by half, it was not significant (Figure 7B).

### 3.6 | Effects of anti-LYVE-1 mAb on primary tumor growth in vivo

We next evaluated whether the purified anti-LYVE-1 mAb were able to inhibit tumor growth of the primary lesion. The 64R mAb significantly suppressed tumor growth by MDA-231 cells compared with control rat IgG (Figure 7C). Furthermore, we found that the anti-LYVE-1 mAb decreased the amount of lymphatic vessels in the tumor lesion derived from MDA-231 cells as compared with that in control mice (Figure 7D).

## 4 | DISCUSSION

Although the metastasis of cancer cells leads to poor prognosis, little is known about its mechanisms. Between the 2 different patterns of

metastasis, the lymphatic route is considered to play a more critical role than the hematogenous route, especially in human carcinomas.<sup>6,7</sup> Therefore, it is important to clarify the mechanism of lymphogenous metastasis to discover novel inhibitors of cancer metastasis. LYVE-1 is specifically expressed in lymphatic vessels,<sup>9,10</sup> but it is unclear whether LYVE-1 is involved in cancer metastasis. In this study, we examined whether LYVE-1 is involved in cancer metastasis and assessed its suitability as a target for cancer therapy.

Prior to this study, we used FCM to select mAb reacting with transfectants expressing GFP-fused target molecules in a GFP-expression-dependent manner as the first screening,<sup>20,21</sup> but this method was difficult for rapid and simultaneous screening of a large number of antibody samples. Given that LYVE-1 is a type 1 single-pass membrane protein, secreted (soluble) proteins can be prepared, as in the case for HER4.<sup>22</sup> We adopted ELISA as the first screening with soluble LYVE-1 proteins, which has a higher throughput than FCM, and can efficiently select specific anti-LYVE-1 mAb. The specificity of the mAb was further confirmed via the second screening with FCM. We finally obtained novel anti-LYVE-1 mAb, 38M, and 64R, which bound to transfectants expressing GFP-fused mouse LYVE-1 in a GFP-expression-dependent manner. Furthermore, on ELISA, neither 38M nor 64R reacted with mouse CD44-fused GFP. Moreover, 38M and 64R were reactive with primary mouse LEC and SVEC4-10 mouse LEC endogenously expressing LYVE-1 proteins. Taken together, we demonstrated 38M and 64R specifically recognize mouse LYVE-1 proteins.

Although 38M and 64R reacted with lymphatic vessels in mouse tissues (Figure 4) but not with blood vessels (Figure 5), several studies have reported LYVE-1 in CD11b- or F4/80-positive macrophages.<sup>33,34</sup> 38M and 64R, however, did not react with thioglycollate-induced macrophages (data not shown), indicating that the epitopes recognized by 38M and 64R are preferentially expressed on the endothelia of lymphatic vessels.

Ascites fluid containing anti-LYVE-1 mAb inhibited metastasis to axillary LN. Moreover, primary tumor formation was also inhibited,



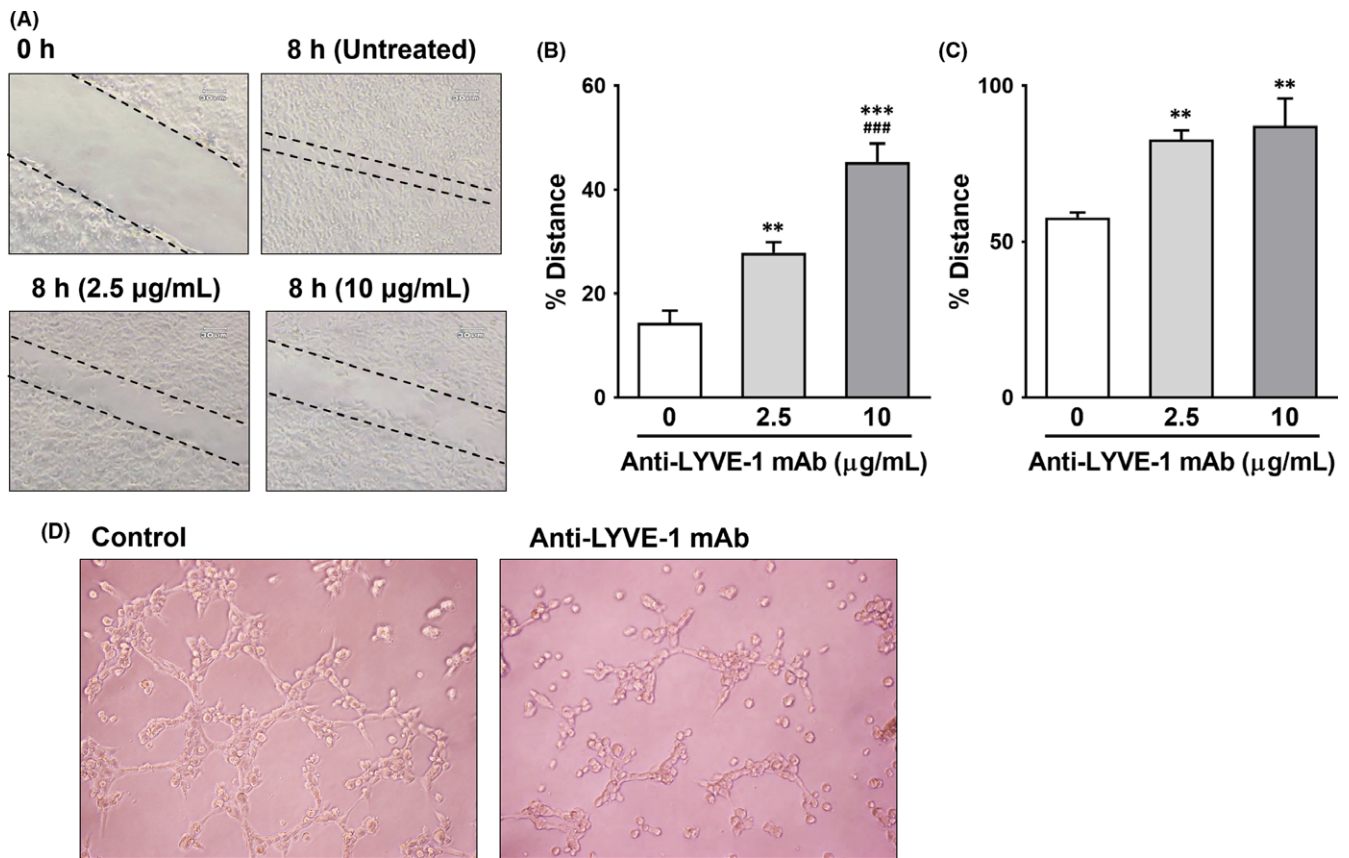


**FIGURE 6** Effects of anti-lymphatic vessel endothelial hyaluronan receptor 1 (anti-LYVE-1) mAb on cell migration and tube formation. A–C, Wound healing assay. A, Representative images of wounds in HEK293 cell culture before and 8 hours after treatment with 64R. Broken lines, wound edge. A,B, HEK293 cells expressing mouse LYVE-1-GFP or C, SVEC4-10 were cultured until 100% confluency. Cells were scratched and treated with supernatants from MDA-MB-231-luc-LN cells. B,C, Distance between the wound edges in B, HEK293F or C, SVEC4-10, expressed as a percentage of the distance before treatment with the mAb. Results are expressed as mean  $\pm$  SEM ( $n = 3$ ).  $**P < .01$ ,  $***P < .001$ , vs without mAb.  $###P < .001$ , vs with mAb concentration 2.5  $\mu\text{g/mL}$ . D, Tube formation assay. SVEC4-10 cells were plated onto Matrigel-coated chambers, and the supernatant from MDA-231 cells was added with or without 64R. Three hours after incubation at 37°C, images were taken using a microscope

although not significantly. In the place of ascites fluid as the mAb source, we used purified mAb in order to clarify the role of LYVE-1 in primary tumor formation. Purified anti-LYVE-1 mAb suppressed primary tumor growth and reduced the number of lymphatic vessels in the primary tumor lesions. Taken together, suppression of primary tumor formation by anti-LYVE-1 mAb is due to the inhibition of lymphangiogenesis in the primary tumor.

A small peptide derived from somatotropin, which acts as a lymphangiogenesis inhibitor, significantly inhibited the migration of highly metastatic cancer cells.<sup>35</sup> Endostatin was also reported to inhibit cell migration and tumor-induced lymphangiogenesis.<sup>36</sup> Furthermore, CXCL1 secreted from LEC was found to be involved in LEC migration and lymphangiogenesis.<sup>37</sup> Therefore, cell migration is closely related to lymphangiogenesis. In this study, we found that inhibition of LYVE-1 using mAb significantly suppressed in vitro cell migration of HEK293F cells expressing LYVE-1 and SVEC4-10 mouse LEC cells. This result, together with the present finding that anti-LYVE-1 mAb inhibit the formation of lymphatic vessels in the primary tumor, suggest that LYVE-1 plays a critical role in lymphangiogenesis.

In the wound healing assay, 64R suppressed the migration of HEK293 cells expressing mouse LYVE-1 and SVEC4-10 mouse LEC induced by the supernatant from MDA-MB-231-Luc-LN cells. In addition, tube formation by SVAC4-10 cells was inhibited by 64R. VEGF is highly expressed in MDA-MB-231-Luc-LN cells,<sup>38</sup> and secretion of VEGF proteins by MDA-231 cells has been reported.<sup>39,40</sup> VEGF has been shown to be involved in lymphangiogenesis and invasion in tumor metastasis.<sup>41,42</sup> Given that lymphangiogenesis occurs during wound healing,<sup>43-45</sup> VEGF likely plays a role in the induction of cell migration in the presence of the supernatant from MDA-231 cells. In this context, VEGF may induce shedding of the LYVE-1 ectodomain, which promoted cell migration.<sup>12</sup> The supernatant did not facilitate the migration of parental HEK293F cells, and the anti-LYVE-1 mAb did not affect the migration of HEK293 cells expressing LYVE-1 in the absence of the MDA-231 cell supernatant (data not shown). Therefore, these results suggest that the interaction between LYVE-1 and VEGF is involved in the migration of LEC. Further experiments are needed to elucidate the exact mechanism of LYVE-1-mediated cell migration, particularly the identification of factors inducing the migration of LEC from MDA-231 cells.

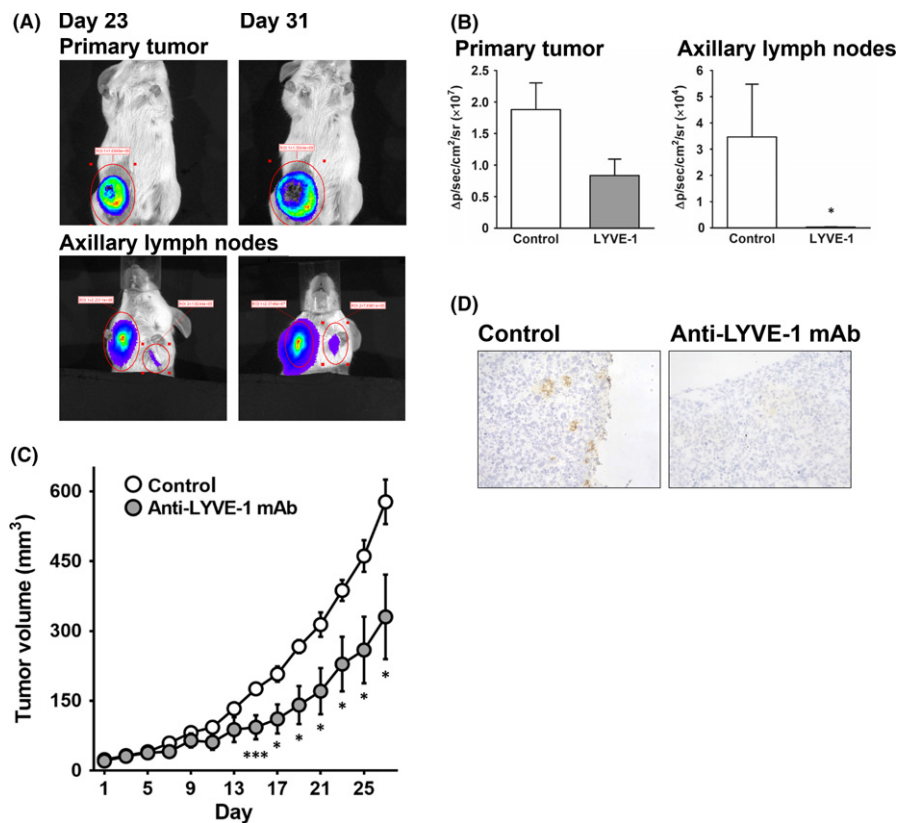


**FIGURE 7** Effects of anti-lymphatic vessel endothelial hyaluronan receptor 1 (anti-LYVE-1) mAb on cancer metastasis and primary tumor growth. A,B, Highly metastatic MDA-MB-231-luc-LN cells were implanted into the mammary fat pads of SCID mice, and tumor metastasis was monitored on bioluminescence imaging. MDA-231 cells in tumors were imaged after luciferin injection with an IVIS instrument. A, Representative images of MDA-231 primary tumor cells grafted onto the right inguinal mammary gland and spontaneous metastasis to axillary lymph nodes in mice 23 and 31 days after inoculation. B, Bioluminescence intensity 52 days after treatment with 64R-containing ascites fluid. C,D, Nude mice were intradermally inoculated with MDA-231 cells. The 64R or isotype control mAb was injected 4 times every 4 days after confirming that the tumors were engrafted. C, Time course of tumor growth; the size of the tumors was periodically measured, and the tumor volume (mm<sup>3</sup>) was calculated by the formula  $0.5 \times (\text{length}) \times (\text{width})^2$ . D, Representative images of primary MDA-231 tumors treated with anti-LYVE-1 or isotype control mAb. Results are expressed as mean  $\pm$  SEM (A,B,  $n = 4$ –5; C,D,  $n = 7$ ). \* $P < .05$ , \*\*\* $P < .001$ , vs control

In this study, the number of lymphatic vessels in primary tumors was reduced by the anti-LYVE-1 mAb. Given that higher expression of LYVE-1 is observed in LEC during embryogenesis<sup>46</sup> and in initial lymphatic vessels in the early postnatal period,<sup>47</sup> it is possible that LYVE-1 functions in lymphangiogenesis. No difference, however in lymphatic vessel density between LYVE-1 knockout mice and wild-type mice has been reported.<sup>48,49</sup> This suggests that the role of LYVE-1 in lymphangiogenesis during early development is different from that under pathological conditions. Although further studies are needed to clarify the function of LYVE-1 in lymphangiogenesis in tumor lesions, the difference in the roles of LYVE-1 between pathological and normal conditions may be due to differences in the expression of LYVE-1 and its ligand. In colorectal cancer, LYVE-1 expression and lymphatic vessel density in tumor or normal tissue adjacent to the tumor are significantly higher than in normal tissue.<sup>50</sup> Increased expression of LYVE-1 has also been reported in gastric cancer<sup>51</sup> and in neuroblastoma.<sup>52</sup> Furthermore, increased LYVE-1 protein expression and LYVE-1-positive lymphatic vessel density in intratumor and marginal regions are associated with a poor

outcome.<sup>52</sup> Regarding the ligands of LYVE-1, fibroblast growth factor 2 (FGF2) directly binds to LYVE-1 with a higher affinity than hyaluronan, and FGF2 induced LEC proliferation and tube formation via LYVE-1.<sup>53</sup> FGF2 was also increased in numerous tumor tissues.<sup>54–57</sup> Given that the inhibition of LEC migration by anti-LYVE-1 occurred only in the presence of the MDA-231 cell supernatant in the present study, the anti-LYVE-1 mAb may exhibit anti-lymphangiogenesis effects under pathological conditions such as tumorigenesis.

Several studies have indicated that drugs and molecules with anti-lymphangiogenesis effects suppress tumor growth. A multiple kinase inhibitor, Foretinib, reduced the lymphatic vessel density in tumors and tumor growth in a xenograft mouse model.<sup>58</sup> Furthermore, overexpression of microRNA-128 decreased the number of lymphatic vessels and tumor volume.<sup>59</sup> Here, we demonstrated that the anti-LYVE-1 mAb reduced the tumor volume in vivo. Therefore, these anti-tumor effects are likely due to the reduction of lymphatic vessels in tumor, which inhibits lymphangiogenesis for primary tumor formation.

In conclusion, anti-LYVE-1 mAb inhibits cancer metastasis and primary tumor formation by suppressing lymphangiogenesis. Together with the knowledge that primary tumors induce lymphatic vessels to create a specific microenvironment before metastasis,<sup>60</sup> this study strongly suggests that inhibition of lymphangiogenesis by anti-LYVE-1 mAb will play an essential role in cancer therapy. Inhibition of hemangiogenesis by anti-VEGF-A has already been adopted for the therapy of several malignancies.<sup>61,62</sup> In this context, inhibition of lymphangiogenesis by anti-LYVE-1 mAb may become a next-generation therapy for human cancers.

## ACKNOWLEDGMENTS

This study was supported by grants to T.M. by the "Academic Frontier" Project (Kindai University, (2005-2007, F000132), MEXT (Ministry of Education, Culture, the "Adaptable and Seamless Technology Transfer Program through R&D" Project (2009-2011, AS2115048G), and a matching fund subsidy-supported Program for the Strategic Research Foundation at Private Universities (2014-2018, S1411037).

## CONFLICT OF INTEREST

The authors declare no conflicts of interest.

## ORCID

Takashi Masuko  <http://orcid.org/0000-0002-2410-2007>

## REFERENCES

- Mehlen P, Puisieux A. Metastasis: a question of life or death. *Nat Rev Cancer*. 2006;6:449-458.
- Nguyen DX, Bos PD, Massagué J. Metastasis: from dissemination to organ-specific colonization. *Nat Rev Cancer*. 2009;9:274-284.
- Monteiro J, Fodde R. Cancer stemness and metastasis: therapeutic consequences and perspectives. *Eur J Cancer*. 2010;46:1198-1203.
- Gupta GP, Massagué J. Cancer metastasis: building a framework. *Cell*. 2006;127:679-695.
- Wong SY, Hynes RO. Lymphatic or hematogenous dissemination: how does a metastatic tumor cell decide? *Cell Cycle*. 2006;5:812-817.
- Clarijs R, Ruiter DJ, de Waal RM. Lymphangiogenesis in malignant tumours: does it occur? *J Pathol*. 2001;193:143-146.
- Pepper MS. Lymphangiogenesis and tumor metastasis: myth or reality? *Clin Cancer Res*. 2001;7:462-468.
- Stacker SA, Baldwin ME, Achen MG. The role of tumor lymphangiogenesis in metastatic spread. *FASEB J*. 2002;16:922-934.
- Banerji S, Ni J, Wang SX, et al. LYVE-1, a new homologue of the CD44 glycoprotein, is a lymph-specific receptor for hyaluronan. *J Cell Biol*. 1999;144:789-801.
- Prevo R, Banerji S, Ferguson DJ, Clasper S, Jackson DG. Mouse LYVE-1 is an endocytic receptor for hyaluronan in lymphatic endothelium. *J Biol Chem*. 2001;276:19420-19430.
- Wu M, Du Y, Liu Y, et al. Low molecular weight hyaluronan induces lymphangiogenesis through LYVE-1-mediated signaling pathways. *PLoS One*. 2014;9:e92857.
- Nishida-Fukuda H, Araki R, Shudou M, et al. Ectodomain shedding of lymphatic vessel endothelial hyaluronan receptor 1 (LYVE-1) is induced by vascular endothelial growth factor A (VEGF-A). *J Biol Chem*. 2016;291:10490-10500.
- Jackson DG, Prevo R, Clasper S, Banerji S. LYVE-1, the lymphatic system and tumor lymphangiogenesis. *Trends Immunol*. 2001;22:317-321.
- Yu M, Zhang H, Liu Y, et al. The cooperative role of S1P3 with LYVE-1 in LMW-HA-induced lymphangiogenesis. *Exp Cell Res*. 2015;336:150-157.
- Langenes V, Svensson H, Börjesson L, et al. Expression of the chemokine decoy receptor D6 is decreased in colon adenocarcinomas. *Cancer Immunol Immunother*. 2013;62:1687-1695.
- Poyet C, Thomas L, Benoit TM, et al. Implication of vascular endothelial growth factor A and C in revealing diagnostic lymphangiogenic markers in node-positive bladder cancer. *Oncotarget*. 2017;8:21871-21883.
- Skobe M, Hawighorst T, Jackson DG, et al. Induction of tumor lymphangiogenesis by VEGF-C promotes breast cancer metastasis. *Nat Med*. 2001;7:192-198.
- Mattila MM, Ruohola JK, Karpanen T, Jackson DG, Alitalo K, Häkkinen PL. VEGF-C induced lymphangiogenesis is associated with lymph node metastasis in orthotopic MCF-7 tumors. *Int J Cancer*. 2002;98:946-951.
- Xiong Y, Brinkman CC, Famulski KS, et al. A robust in vitro model for trans-lymphatic endothelial migration. *Sci Rep*. 2017;7:1633.
- Ohno Y, Suda K, Masuko K, Yagi H, Hashimoto Y, Masuko T. Production and characterization of highly tumor-specific rat monoclonal antibodies recognizing the extracellular domain of human L-type amino-acid transporter 1. *Cancer Sci*. 2008;99:1000-1007.
- Masuko T, Ohno Y, Masuko K, et al. Towards therapeutic antibodies to membrane oncoproteins by a robust strategy using rats immunized with transfectants expressing target molecules fused to green fluorescent protein. *Cancer Sci*. 2011;102:25-35.
- Okazaki S, Nakatani F, Masuko K, et al. Development of an ErbB4 monoclonal antibody that blocks neuregulin-1-induced ErbB4 activation in cancer cells. *Biochem Biophys Res Commun*. 2016;470:239-244.
- Ishimoto T, Oshima H, Oshima M, et al. CD44<sup>+</sup> slow-cycling tumor cell expansion is triggered by cooperative actions of Wnt and prostaglandin E<sub>2</sub> in gastric tumorigenesis. *Cancer Sci*. 2010;101:673-678.
- Yae T, Tsuchihashi K, Ishimoto T, et al. Alternative splicing of CD44 mRNA by ESRP1 enhances lung colonization of metastatic cancer cell. *Nat Commun*. 2012;3:883.
- Pham TH, Baluk P, Xu Y, et al. Lymphatic endothelial cell sphingosine kinase activity is required for lymphocyte egress and lymphatic patterning. *J Exp Med*. 2010;207:17-27.
- Yegutkin GG, Auvinen K, Rantakari P, et al. Ecto-5'-nucleotidase/CD73 enhances endothelial barrier function and sprouting in blood but not lymphatic vasculature. *Eur J Immunol*. 2015;45:562-573.
- Walter-Yohrling J, Morgenbesser S, Rouleau C, et al. Murine endothelial cell lines as models of tumor endothelial cells. *Clin Cancer Res*. 2004;10:2179-2189.
- Tanaka T, Kitamura F, Nagasaka Y, Kuida K, Suwa H, Miyasaka M. Selective long-term elimination of natural killer cells in vivo by an anti-interleukin 2 receptor  $\beta$  chain monoclonal antibody in mice. *J Exp Med*. 1993;178:1103-1107.
- Stacker SA, Williams SP, Karnezis T, Shayan R, Fox SB, Achen MG. Lymphangiogenesis and lymphatic vessel remodelling in cancer. *Nat Rev Cancer*. 2014;14:159-172.
- Sleeman JP, Thiele W. Tumor metastasis and the lymphatic vasculature. *Int J Cancer*. 2009;125:2747-2756.
- Alitalo K. The lymphatic vasculature in disease. *Nat Med*. 2011;17:1371-1380.
- Fang C, Miguel MA, Avis I, Martinez A, Zudaire E, Cuttitta F. Non-peptide small molecule regulators of lymphangiogenesis. *Lymphat Res Biol*. 2009;7:189-196.
- Cho CH, Koh YJ, Han J, et al. Angiogenic role of LYVE-1-positive macrophages in adipose tissue. *Circ Res*. 2007;100:e47-e57.

34. Zheng M, Kimura S, Nio-Kobayashi J, Takahashi-Iwanaga H, Iwanaga T. Three types of macrophagic cells in the mesentery of mice with special reference to LYVE-1-immunoreactive cells. *Biomed Res.* 2014;35:37-45.
35. Lee E, Rosca EV, Pandey NB, Popel AS. Small peptides derived from somatotropin domain-containing proteins inhibit blood and lymphatic endothelial cell proliferation, migration, adhesion and tube formation. *Int J Biochem Cell Biol.* 2011;43:1812-1821.
36. Zhuo W, Luo C, Wang X, Song X, Fu Y, Luo Y. Endostatin inhibits tumour lymphangiogenesis and lymphatic metastasis via cell surface nucleolin on lymphangiogenic endothelial cells. *J Pathol.* 2010;222:249-260.
37. Xu J, Zhang C, He Y, et al. Lymphatic endothelial cell-secreted CXCL1 stimulates lymphangiogenesis and metastasis of gastric cancer. *Int J Cancer.* 2012;130:787-797.
38. Zibara K, Awada Z, Dib L, et al. Anti-angiogenesis therapy and gap junction inhibition reduce MDA-MB-231 breast cancer cell invasion and metastasis *in vitro* and *in vivo*. *Sci Rep.* 2015;5:12598.
39. Li C, Guo S, Shi T. Role of NF- $\kappa$ B activation in matrix metalloproteinase 9, vascular endothelial growth factor and interleukin 8 expression and secretion in human breast cancer cells. *Cell Biochem Funct.* 2013;31:263-268.
40. Yang H, Wang B, Wang T, et al. Toll-like receptor 4 prompts human breast cancer cells invasiveness via lipopolysaccharide stimulation and is overexpressed in patients with lymph node metastasis. *PLoS One.* 2014;9:e109980.
41. Mandriota SJ, Jussila L, Jeltsch M, et al. Vascular endothelial growth factor-C-mediated lymphangiogenesis promotes tumour metastasis. *EMBO J.* 2001;20:672-682.
42. Krishnan J, Kirkin V, Steffen A, et al. Differential *in vivo* and *in vitro* expression of vascular endothelial growth factor (VEGF)-C and VEGF-D in tumors and its relationship to lymphatic metastasis in immunocompetent rats. *Cancer Res.* 2003;63:713-722.
43. Paavonen K, Puolakkainen P, Jussila L, Jahkola T, Alitalo K. Vascular endothelial growth factor receptor-3 in lymphangiogenesis in wound healing. *Am J Pathol.* 2000;156:1499-1504.
44. Martínez-Corral I, Olmeda D, Diéguez-Hurtado R, Tammela T, Alitalo K, Ortega S. *In vivo* imaging of lymphatic vessels in development, wound healing, inflammation, and tumor metastasis. *Proc Natl Acad Sci USA.* 2012;109:6223-6228.
45. Zampell JC, Yan A, Avraham T, Daluvoy S, Weitman ES, Mehrara BJ. HIF-1 $\alpha$  coordinates lymphangiogenesis during wound healing and in response to inflammation. *FASEB J.* 2012;26:1027-1039.
46. Wigle JT, Harvey N, Detmar M, et al. An essential role for Prox1 in the induction of the lymphatic endothelial cell phenotype. *EMBO J.* 2002;21:1505-1513.
47. Mäkinen T, Adams RH, Bailey J, et al. PDZ interaction site in ephrinB2 is required for the remodeling of lymphatic vasculature. *Genes Dev.* 2005;19:397-410.
48. Gale NW, Prevo R, Espinosa J, et al. Normal lymphatic development and function in mice deficient for the lymphatic hyaluronan receptor LYVE-1. *Mol Cell Biol.* 2007;27:595-604.
49. Luong MX, Tam J, Lin Q, et al. Lack of lymphatic vessel phenotype in LYVE-1/CD44 double knockout mice. *J Cell Physiol.* 2009;219:430-437.
50. Gao F, Lu YM, Cao ML, Liu YW, He YQ, Wang Y. Expression and quantification of LYVE-1 in human colorectal cancer. *Clin Exp Med.* 2006;6:65-71.
51. Ozmen F, Ozmen MM, Ozdemir E, et al. Relationship between LYVE-1, VEGFR-3 and CD44 gene expressions and lymphatic metastasis in gastric cancer. *World J Gastroenterol.* 2011;17:3220-3228.
52. Ramani P, Dungwa JV, May MT. LYVE-1 upregulation and lymphatic invasion correlate with adverse prognostic factors and lymph node metastasis in neuroblastoma. *Virchows Arch.* 2012;460:183-191.
53. Platonova N, Miquel G, Regenfuss B, et al. Evidence for the interaction of fibroblast growth factor-2 with the lymphatic endothelial cell marker LYVE-1. *Blood.* 2013;121:1229-1237.
54. Relf M, LeJeune S, Scott PA, et al. Expression of the angiogenic factors vascular endothelial cell growth factor, acidic and basic fibroblast growth factor, tumor growth factor beta-1, platelet-derived endothelial cell growth factor, placenta growth factor, and pleiotrophin in human primary breast cancer and its relation to angiogenesis. *Cancer Res.* 1997;57:963-969.
55. Giri D, Ropiquet F, Ittmann M. Alterations in expression of basic fibroblast growth factor (FGF) 2 and its receptor FGFR-1 in human prostate cancer. *Clin Cancer Res.* 1999;5:1063-1071.
56. Marzioni D, Lorenzi T, Mazzucchelli R, et al. Expression of basic fibroblast growth factor, its receptors and syndecans in bladder cancer. *Int J Immunopathol Pharmacol.* 2009;22:627-638.
57. Chen Y, Li X, Yang H, et al. Expression of basic fibroblast growth factor, CD31, and  $\alpha$ -smooth muscle actin and esophageal cancer recurrence after definitive chemoradiation. *Tumour Biol.* 2014;35:7275-7282.
58. Chen HM, Tsai CH, Hung WC. Foretinib inhibits angiogenesis, lymphangiogenesis and tumor growth of pancreatic cancer *in vivo* by decreasing VEGFR-2/3 and TIE-2 signaling. *Oncotarget.* 2015;6:14940-14952.
59. Hu J, Cheng Y, Li Y, et al. MicroRNA-128 plays a critical role in human non-small cell lung cancer tumorigenesis, angiogenesis and lymphangiogenesis by directly targeting vascular endothelial growth factor-C. *Eur J Cancer.* 2014;50:2336-2350.
60. Hirakawa S. From tumor lymphangiogenesis to lymphvascular niche. *Cancer Sci.* 2009;100:983-989.
61. Lauro S, Onesti CE, Righini R, Marchetti P. The use of bevacizumab in non-small cell lung cancer: an update. *Anticancer Res.* 2014;34:1537-1545.
62. Qu CY, Zheng Y, Zhou M, et al. Value of bevacizumab in treatment of colorectal cancer: a meta-analysis. *World J Gastroenterol.* 2015;21:5072-5080.

**How to cite this article:** Hara Y, Torii R, Ueda S, et al. Inhibition of tumor formation and metastasis by a monoclonal antibody against lymphatic vessel endothelial hyaluronan receptor 1. *Cancer Sci.* 2018;109:3171–3182. <https://doi.org/10.1111/cas.13755>